Rhubarb and Astragalus Capsule Attenuates Renal Interstitial Fibrosis in Rats with Unilateral Ureteral Obstruction by Alleviating Apoptosis through Regulating Transforming Growth Factor beta1 (TGF-β1)/p38 Mitogen-Activated Protein Kinases (p38 MAPK) Pathway

Authors' Contribution:
Study Design A
Data Collection B
Statistical Analysis C
Data Interpretation D
Manuscript Preparation E
Literature Search F
Funds Collection G

E 1 Xian Zeng*
B 1 Guozhen Cai*
D 1 Taolin Liang
F 1 Qingqing Li
A 1 Yufang Yang
G 2 Xiaobin Zhong
C 1 Xiaoqin Zou
B 1 Mengyuan Qin
F 1 Zhengcheng Mi

1 Department of Pharmacy, The First Affiliated Hospital of Guangxi Medical University, Nanning, Guangxi, P.R. China
2 Regenerative Medicine Research Center, Guangxi Medical University, Nanning, Guangxi, P.R. China

* Xian Zeng and Guozhen Cai contributed equally to this work and should be considered co-first author
Corresponding Authors: Yufang Yang, e-mail: yyf_69@163.com, Xiaobin Zhong, e-mail: 1878125675@qq.com
Source of support: This work was supported by the National Nature Science Foundation of China (No: 81560729, No: 81260598), the Guangxi Natural Science Foundation (No: 2017GXNSFAA198262, No: 2018GXNSFAA294043), the Guangxi Medical and Health Appropriate Technology Development and Application Project (No: S2017016)

Background: Rhubarb and astragalus capsule (RAC) has been used in the clinical treatment of chronic kidney disease for decades. However, the mechanism of RAC has not been fully elucidated. This study aimed to investigate the protective effect and mechanisms of RAC on unilateral ureteral obstruction (UUO)-induced renal interstitial fibrosis.

Material/Methods: The main components of RAC are detected by high-performance liquid phase (HPLC). A rat model of UUO was established, and a subset of rats underwent treatment with RAC. Renal function and renal pathology were examined at 14 days and 21 days after the UUO operation. Renal cell apoptosis was detected by TUNEL staining. The levels of Bcl-2 and Bax in the kidney were examined by western blotting, and the levels of collagen I, α-SMA, transforming growth factor (TGF)-β1, and p38 MAPK in the kidneys were detected by immunohistochemistry.

Results: High-performance liquid phase chromatography showed that RAC contained 1.12 mg/g aloe-emodin, 2.25 mg/g rhein, 1.75 mg/g emodin, and 4.50 mg/g chrysophanol. Administration of RAC significantly decreased the levels of urinary N-acetyl-β-D-glucosaminidase (NAG), serum blood urea nitrogen (BUN), and creatinine (Scr) and also reduced renal tissue damages and interstitial fibrosis induced by UUO in rats. Moreover, the increased levels of collagen I, α-SMA, TGF-β1, p38 MAPK, and the Bax/Bcl-2 ratio, as well as cell apoptosis in the kidney, were induced by UUO, and were all found deceased by RAC treatment.

Conclusions: RAC can improve the renal interstitial fibrosis induced by UUO, and the mechanism may be related to inhibition of renal tubular cell apoptosis via TGF-β1/p38 MAPK pathway.

MeSH Keywords: Apoptosis Regulatory Proteins • p38 Mitogen-Activated Protein Kinases • Renal Insufficiency, Chronic • Transforming Growth Factor beta1

Full-text PDF: https://www.medscimonit.com/abstract/index/idArt/920720

📄 4322   ▦ —   📊 8   📚 53

Background

Chronic kidney disease (CKD) has high morbidity and mortality worldwide. According to the 2013 Global Disease Burden Study, about 956 200 people died of chronic kidney disease [1]. Renal interstitial fibrosis (RIF) is the main pathological feature of CKD. Inhibition of renal interstitial fibrosis may be a critical factor in delaying the progression of CKD. However, the mechanism of RIF is not precise. Some Chinese medicines have been reported to have a prominent effect on RIF [2–4].

Rhubarb and astragalus capsule (RAC) is a commercial product that has been used for decades in the clinic to treat CKD, i.e., chronic renal insufficiency, azotemia, and uremia. This drug is made from the crushed and treated dry powder of the root of medical plants rhubarb (*Rheum palmatum L.*) and astragalus (*Astragalus membranaceus*). As an important medicinal plant, rhubarb has been used to treat diseases due to its dramatic effects of catharsis, anti-fever, anti-infection, anti-inflammation, and even anti-cancer in China throughout history [5]. The other medicinal plant, astragalus, is also known to have some medical values, including promoting diuresis and improving immunity [6]. Our previous study has demonstrated that, by combing the therapeutic properties of the 2 major components, RAC can protect kidney function and has excellent clinical efficacy [7]. However, its mechanism of action has not been fully clarified.

The pathogenesis of RIF is the excessive production and deposition of the extracellular matrix (ECM) [8]. Transforming growth factor (TGF)-β1 is an important cytokine that promotes the progression of renal interstitial fibrosis [9]. TGF-β1 plays a crucial role in the excessive deposition of ECM [10,11]. Other reports have shown that p38 MAPK plays a vital role in the development of renal inflammation and fibrosis [12,13], and inhibition of p38 MAPK protein expression can improve renal fibrosis [12,14]. Therefore, inhibition of p38 MAPK or TGF-β1 protein expression may be an effective strategy to attenuate renal interstitial fibrosis. Interestingly, rhubarb and astragalus have been reported to downregulate the expression of TGF-β1 or inhibit the p38 MAPK signaling pathway [15–17], thereby improving the fibrosis of the kidney and peritoneum [18–21]. This study investigated the effect and mechanism of RAC on protecting RIF through inhibiting apoptosis and TGF-β1/p38 MAPK pathway.

Material and Methods

Reagent

RAC was purchased from the Pharmaceutical Preparation Room of the First Affiliated Hospital of Guangxi Medical University (20150713).

High-performance liquid chromatography (HPLC) analysis

RAC capsules consist of 2 kinds of traditional Chinese medicine powders, rhubarb and *Astragalus membranaceus*. High-performance liquid phase chromatography (HPLC) approach was applied for the major composition analysis of components within the RAC capsules, according to several previous studies [22–24]. To prepare the samples for HPLC analysis, the RAC was processed through a series of treatment steps. Briefly, RAC powder was separated from each individual capsule and transferred into a conical flask, followed by mixing with precisely 50 mL of methanol. The mixture was refluxed and boiled for 1 hour, then filtered through 0.25 μm filter paper. The 15 mL of filtrate was dried using a rotary evaporation, and 25 mL of 8% hydrochloric acid (HCl) solution was added to redissolve the filtrate under ultrasonication for 2 minutes. An addition of 20 mL chloroform was mixed with the sonicated filtrate and refluxed for another 1 hour. The chloroform phase was recovered and further extracted with 10 mL extra chloroform for 3 times. Totally, 50 mL of the chloroform phase was collected and dried. The dry residue was dissolved in a small amount of methanol, transferred into a 10 mL-size brown volumetric flask and brought to volume by methanol. The processed samples were submitted to a Shimadzu system (LC-20A, Japan) for HPLC analysis. The system comprised a binary pump (LC-20 AT), a photodiode array detector (SPD-M20A), and an auto-sampler (SLC-20A). A Welchrom C18 (250×4.6 mm, 5 μm, Waters) column was used, and the detection wavelengths were set at 254 nm. The column thermostat was maintained at 35°C. Mobile phase A was methanol (TEDIA, USA), and mobile phase B was water containing 0.1% phosphoric acid (Kermel, Chemio Chemical Reagent Co., Ltd., Tianjin, China). The elution profile was: 0~70 minutes, 50~75% A; 70~90 minutes, 75% A. The flow rate was 1.00 mL/minute, and the injection volume was 20 μL.

Animals

One hundred clean grade male Sprague-Dawley (SD) rats (250±20 g) were purchased from the Experimental Animal Center of Guangxi Medical University (Guangxi, China Permit No.: SCXK20140003). The animal care and experiments were conducted according to protocols approved by the institutional ethics committee of Guangxi Medical University.

Experimental design

The rats were divided randomly into the following 5 groups according to our experimental design: 1) Sham group: rats were gavaged twice daily with the same volume of saline as RAC. 2) UUO (unilateral ureteral obstruction) group, rats were gavaged twice daily with the same amount of saline as RAC. 3) UUO+L-RAC group, which were gavaged twice daily with a low dose of RAC (81.46 mg/kg). 4) UUO+M-RAC group: rats were

gavaged twice daily with a medium dose of RAC (162.93 mg/kg). 5) UUO+H-RAC group: rats were gavaged twice daily with a high dose of RAC (325.86 mg/kg). All rats were dosed after 7 days post-surgery, with a duration of 7 days or 14 days. Among them, the dose of the UUO+M-RAC group was converted from the clinical treatment commonly used in adults to the rat dose.

The surgery of UUO was performed. After an intraperitoneal injection of 10% chloral hydrate (350 mg/kg) was received, the left ureter was exposed. Then the 2 ends of ureter were ligated with 6-0 silk sutures. Finally, the ureter between the 2 ligatures was cut and removed, and the abdomen was sutured. The surgery of the Sham group was performed all steps of UUO-procedure except ligation and cut of the ureter. Surgery strictly abides by the aseptic technique.

Biological sample collection

Collection of biological samples from the experimental animals were following our previous procedure [25]. Briefly, venous blood and urine were sampled from 10 rats randomly obtained individuals of each group at 14 days and 21 days after treatments, respectively. The animals were then sacrificed by intraperitoneal injection of chloral hydrate (350 mg/kg bodyweight). The serum was separated from the coagulated blood by centrifugation. Serum and urine samples were immediately stored at –80°C for further analyses. The left kidney (undergone UUO operation) was cleaned *ex vivo* with sterile pre-cold saline. A piece of renal tissue was dissected, one part of this tissue immediately fixed in 4% formaldehyde and embedded by paraffin for histological or histochemical analyses, and the rest of the tissue was kept at –80°C for protein extraction.

Quantitation for BUN, Scr and NAG

To assess the injury of kidney, the levels of serum blood urea nitrogen (BUN) and creatinine (Scr), as well as the level of urinary N-acetyl-β-D-glucosaminidase (NAG), were detected by corresponding commercial kits (C013-1 for BUN, C011-1 for Scr, A031 for NAG; Nanjing Jiancheng Bioengineering Research Institute, Nanjing, China) respectively.

Hematoxylin and eosin (H&E) staining

To assess tubulointerstitial injury, the paraffin-embedded renal sections were sliced into 3 μm thickness and stained with hematoxylin and eosin (H&E) dyes. Renal histology was examined using an Olympus microscope (Olympus IX51, Japan). The tubulointerstitial injury level was evaluated by reference to the published tubulointerstitial injury scoring standard [26], based on observation of 10 randomly selected and non-overlapping vision fields (400×). The mean score was then calculated and compared among the groups.

Masson staining

Masson staining method was used to assess renal interstitial fibrosis level by using a Masson trichromic kit (ab150669, Abcam, USA). After the staining processes, the renal slices were observed and photographed under an Olympus microscope (Olympus IX51, Japan). The area of blue-stained regions (representing fibrosis) was then measured by the Image Pro-plus 6.0 (Olympus Soft Imaging Solutions, Germany). The average area of kidney interstitial fibrosis was compared among the groups.

Immunohistochemical analyses for type I collagen, α-SMA, TGF-β1 and, p38 MAPK proteins

The sliced renal tissue was first processed for immunohistochemistry by following the routine processes (dewaxed, dehydrated and, microwaved for antigen retrieval in turn). 5% bovine serum albumin (BSA) buffer (v/v in phosphate-buffered saline) following 0.3% hydrogen peroxide (v/v in water) was used to block any possible nonspecific binding. The expression of type I collagen, α-SMA, TGF-β1, or p38 MAPK proteins were primarily labeled with rabbit anti-rat collagen I antibody (1: 1000 dilution; Abcam, Cambridge, UK), rabbit anti-rat α-SMA antibody (1: 600 dilution; Abcam, Cambridge, UK), rabbit anti-rat TGF-β1 antibody (1: 2000 dilution; Abcam, Cambridge, UK) or rabbit anti-rat p38 MAPK antibody (1: 2000 dilution; CST, Boston, US) overnight at 4°C, respectively. The primary antibody binding was then localized by incubation with biotinylated secondary IgG and developed using the DAB (3, 3'-diaminobenzidine) kit (Boster, Wuhan, China). Observation and image acquisition were performed under an Olympus microscope. The integrated optical density (IOD) of the positively stained area was quantitated and analyzed using Image-Pro software, based on 10 randomly chosen fields (400×) of each slice. Mean IOD for each sample was calculated. The protein expression was presented as mean IOD/mean positive stained areas.

TUNEL assay for renal cell apoptosis

TUNEL assay was performed to detect the cellular apoptosis in the kidney tissue. A Roche In Situ Cell Death Detection Kit (Roche Diagnostics, Penzberg, Germany) was employed according to the manufacturer's instructions. Briefly, the tissue slices were deparaffinized then incubated with 10 g/mL of proteinase K for 15 minutes at room temperature, followed by immersing into terminal deoxynucleotidyl transferase-labelling reaction mixture for 1.5 hours. After certain rinses, the slices were incubated with anti-FITC-horseradish peroxidase conjugate for 30 minutes in a 37°C incubator in the dark. DAB (Boster, Wuhan, China) was then used for coloring development. The TUNEL-positive cells were counted and photographed were taken by the imaging analysis system (Olympus Soft Imaging Solutions, Germany).

Western blotting for Bax and Bcl-2

Total protein of rat kidney tissue from different groups was prepared by liquid-nitrogen grinding with RIPA lysis buffer (Beyotime, Shanghai, China) containing 1% (v/v) of phosphatase inhibitor (100×) (CWBio, Beijing, China). The protein lysates were quantified by BCA Protein Assay Kit (Beyotime, Shanghai, China) according to the manufacturer's instruction. The samples were separated on 12% SDS-PAGE at 80V for 2 hours, transferred to polyvinylidene difluoride (PVDF) membrane (Millipore, Billerica, USA) at 100 mA for 1 hour then blocked by QuickBlock™ Blocking Buffer (Beyotime, Shanghai, China), and analyzed by western blotting analysis using Bcl-2 antibody (rabbit anti-rat monoclonal; 1: 1000 dilution; CST, Danvers, USA) or Bax (D3R2M) rabbit mAb (Rodent Preferred; 1: 1000 dilution; CST, Danvers, USA) as the primary antibody and DyLight™ 680 conjugate anti-rabbit IgG (H+L) (1: 15000 dilution; CST, Danvers, USA) as the secondary antibody. The result was analyzed by the Odyssey infrared fluorescence scanning imaging system (Odyssey, LICOR, USA). Rabbit recombinant monoclonal GAPDH antibody (1: 10000 dilution; Abcam, Cambridge, USA) was used as an internal control.

Statistical analysis

Statistical analysis was performed using SPSS software, version 17.0 (SPSS, Inc., Chicago, IL, USA). The data were expressed as the mean±standard deviation (SD). The statistical significance of differences was calculated using the one-way analysis of variance (ANOVA), and $P<0.05$ was considered statistically significant.

Results

Composition analysis of RAC

HPLC analyzed the main components of RAC, and the results were as follows: aloe-emodin, rhein, emodin, and chrysophanol were 1.12 mg/g, 2.25 mg/g, 1.75 mg/g, and 4.50 mg/g, respectively (Figure 1A, 1B).

RAC reduced Scr, BUN and urinary NAG levels in UUO rats.

The rats in the UUO group showed higher (BUN, Scr, and NAG levels at 14 days and 21 days compared to the Sham group (Figure 2). However, UUO+M-RAC group and UUO+H-RAC group showed lower BUN and NAG at 14 days and 21 days as well as reduced Scr at 21 days compared to UUO group (Figure 2).

Additionally, the UUO+H-RAC group showed lower BUN and NAG levels at 21 days than that of the UUO+L-RAC group and UUO+M-RAC group ($P<0.05$).

RAC attenuated UUO-induced renal tissue damage

H&E stained showed significant pathological changes in the UUO group at 14 days, including tubular dilatation, protein exudation, inflammatory cell infiltration, proximal convoluted tubule edema, and increased renal damage at 21 days (Figure 3A). The RAC treatment groups exhibited fewer kidney damages than the UUO group, of which UUO+H-RAC showed the least kidney damages (Figure 3A).

Additionally, higher tubulointerstitial injury scores were observed in the UUO group at 14 days and 21 days compared to the Sham group. Conversely, compared with the UUO group, the RAC treatment groups had lower renal tubulointerstitial injury scores at 14 days (Figure 3B) and 21 days (Figure 3C). Moreover, the tubulointerstitial injury scores of the UUO+H-RAC group and the UUO+M-RAC group were significantly lower than the scores of the UUO+L-RAC group at the same time point. The renal tubulointerstitial injury scores were significantly lower in the UUO+L-RAC group and the UUO+M-RAC group at 21 days than that at 14 days.

RAC reduced UUO-induced renal fibrosis

Masson stained of renal samples showed that the Sham group had no renal interstitial fibrosis, while renal interstitial fibrosis was found in the UUO group at 14 days, and aggravated at 21 days (Figure 4A). Importantly, the renal interstitial fibrosis was dramatically decreased in the RAC treatment groups compared with the UUO group at 14 days (Figure 4B) and 21 days (Figure 4C).

RAC decreased the renal α-SMA level induced by UUO

The renal α-SMA level was analyzed by immunohistochemistry. The α-SMA protein was mainly expressed in renal tubular epithelial cells. The UUO group showed increased renal α-SMA expression compared to the Sham group (Figure 5A, 5C). Additionally, the renal α-SMA level was decreased significantly in the UUO+M-RAC group and the UUO+ H-RAC group compared to the UUO group at 14 days (Figure 5A, 5C). The renal α-SMA level was decreased significantly in all RAC treatment groups compared to the UUO group at 21 days (Figure 5A, 5C).

The α-SMA level in UUO+ H-RAC group at 21 days was significantly lower than that at 14 days (Figure 5A, 5C).

RAC decreased the renal collagen I level induced by UUO

The renal collagen I level was analyzed by immunohistochemistry. The collagen I protein was mainly expressed in the cytoplasm of renal tubular epithelial cells. Additionally, the renal collagen I level in the UUO group was significantly
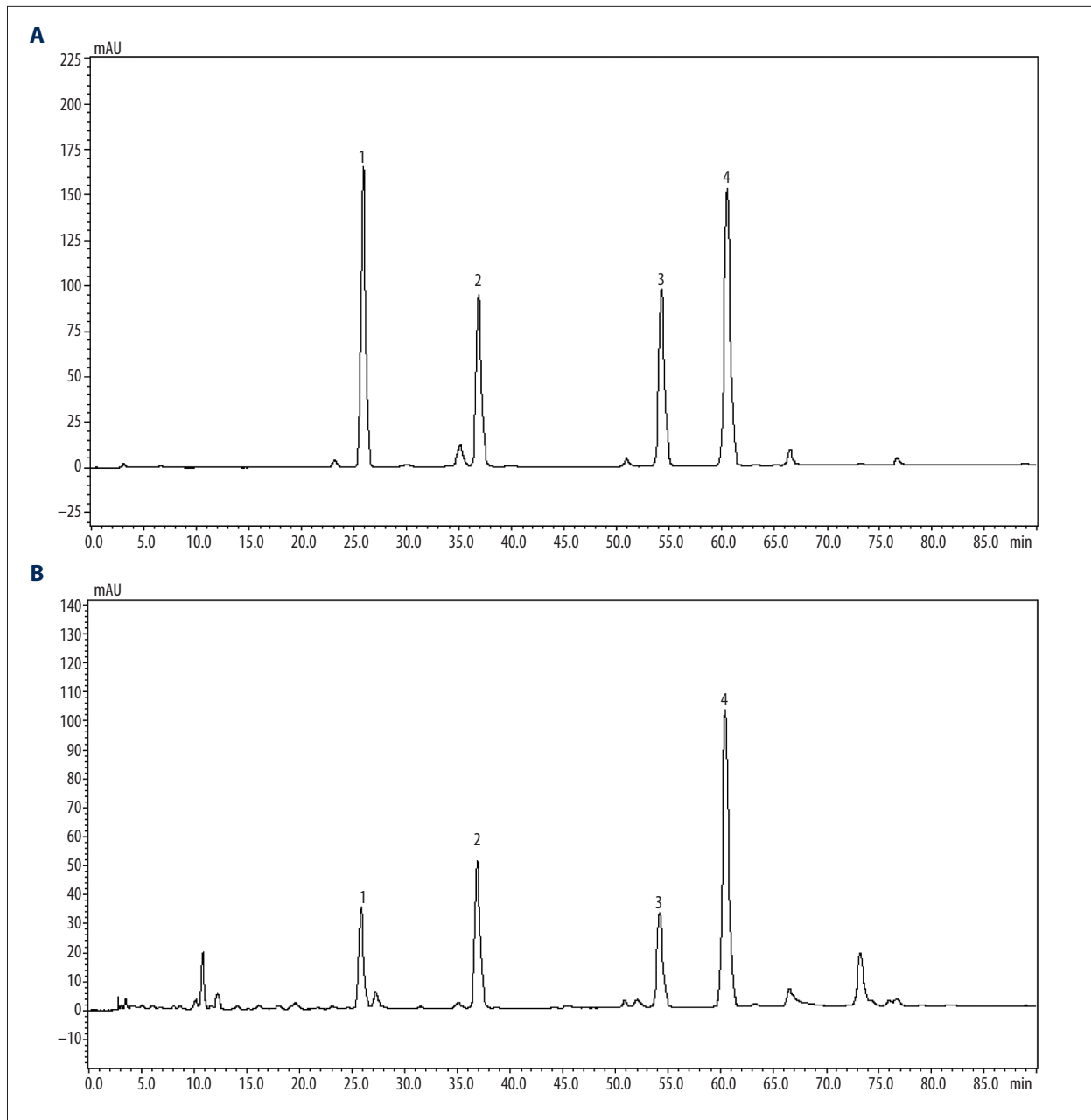
Figure 1. High-performance liquid chromatography of the RAC extract. HPLC analysis of RAC extract was performed using a Shimadzu system. The mobile phase consisted of solvents (**A**) methanol and (**B**) 0.1% phosphoric acid, run at a flow rate of 1.00 mL/minutes. Elution condition whereas follows 0~70 minutes, 50~75% A; 70~90 minutes, 75% A. The sample injection volume was 20 μL. (**A**) HPLC peaks for standard reference substances, including aloe-emodin, rhein, emodin, and chrysophanol (left to right in order). (**B**) HPLC peaks for testing sample (RAC). Optimum HPLC separation was achieved at 35°C and monitored at 254 nm. AU – arbitrary units; RAC – rhubarb and astragalus capsule; HPLC – high-performance liquid chromatography.

increased compared to the Sham group at 14 days and 21 days (Figure 5B, 5D). Moreover, the renal collagen I level was decreased significantly in the UUO+M-RAC group and the UUO+H-RAC group compared to the UUO group at 14 days, and it was decreased dramatically in all RAC treatment groups compared to the UUO group at 21 days (Figure 5B, 5D).

The collagen I level in the UUO+M-RAC group and the UUO+H-RAC group at 21 days were significantly lower than those at 14 days (*P*<0.05).
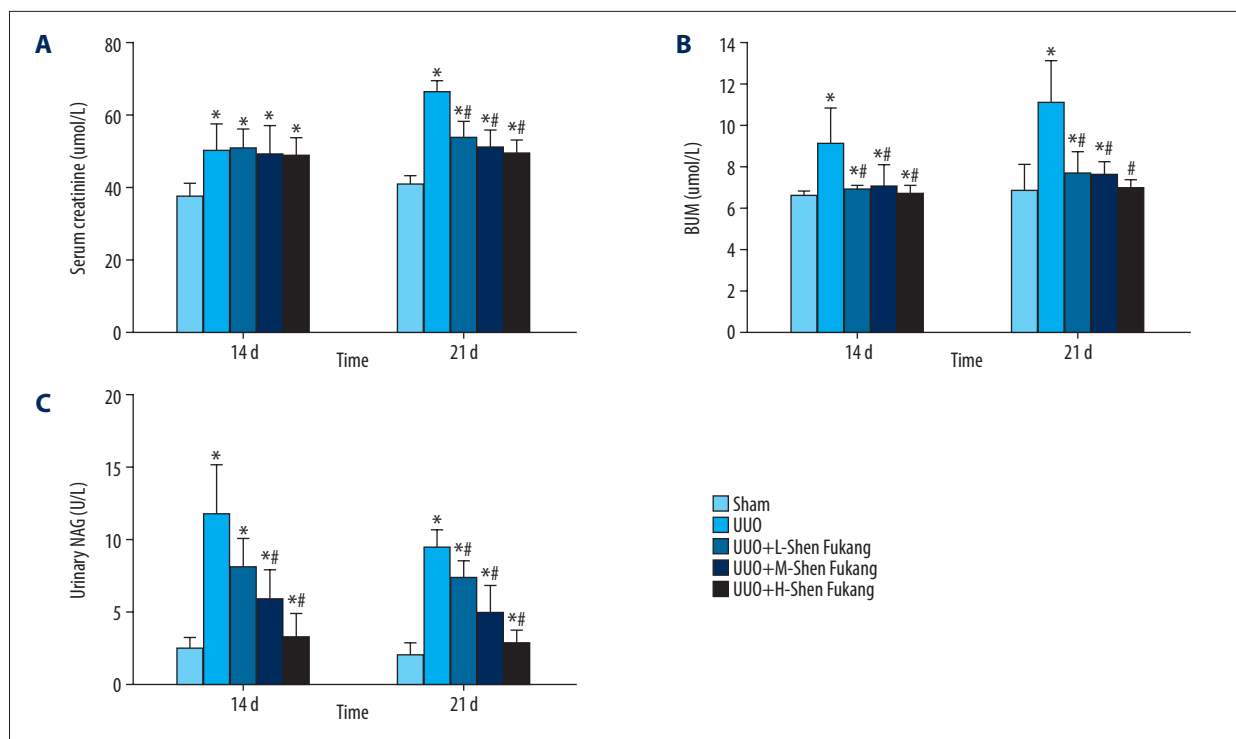
Figure 2. Serum creatinine, BUN and urinary NAG levels in rats after 14 days and 21 days of UUO or sham-operation treatment. Healthy male rats were grouped randomly (n=10 in each group) and UUO model or sham model surgically established. Equal volume of high (H, 325.86 mg/kg body weight), medium (M, 162.93 mg/kg body weight) or low (L, 81.46 mg/kg body weight) dose of RAC as the treatment, was infused to stomach of the UUO rats twice daily by 7 days post-surgery, while equal volume of sterile saline was given that served as the untreated control group (UUO group). Rats received sham-surgery and gavaged with an equal volume of saline were set as the Sham group. After 14- or 21-days post-surgery (7 or 14 days after the RAC treatments), blood and urine were obtained and centrifuged. BUN, Scr, and urinary NAG levels were detected using the corresponding assay kits. (**A**) Scr, (**B**) BUN, and (**C**) urinary NAG levels in the Sham, UUO, UUO+L-RAC, UUO+M-RAC and UUO+H-RAC groups of rats are shown. Data are represented as mean±SD (n=10). * $P<0.05$ compared with the Sham group, # $P<0.05$ compared with UUO group. BUN – blood urea nitrogen; Scr – serum creatinine; NAG – N-acetyl-β-D-glucosaminidase; RAC – rhubarb and astragalus capsule; UUO – unilateral ureteral obstruction; SD – standard deviation.

RAC inhibited renal cells apoptosis induced by UUO

The apoptosis rate of renal samples was detected by TUNEL stained. As shown in Figure 6, the apoptosis rate was significantly increased in the UUO group when compared with the Sham group at 14 days and 21 days (Figure 6). Importantly, the apoptosis rate of renal samples was dramatically decreased in the UUO+M-RAC group and the UUO+H-RAC group when compared with the UUO group at 14 days (Figure 6B) and 21 days (Figure 6C).

RAC decreased the renal Bax level induced by UUO

The level of Bax protein in renal samples was no significant difference between 14 days and 21 days in the Sham group. Besides, the level of Bax protein in renal tissues was significantly increased in the UUO group compared with the Sham group at 14 days and 21 days (Figure 7A, 7B). Moreover, the level of Bax protein in renal tissues decreased significantly in

RAC treatment groups when compared with the UUO group at 14 days and 21 days ($P<0.05$).

The levels of Bax in renal tissues of RAC treatment groups were significantly decreased at 21 days than those at 14 days ($P<0.05$), while there was no significant difference among these 3 groups treated with RAC (Figure 7A, 7B).

RAC increased the renal Bcl-2 level induced by UUO

In contrast, the renal Bcl-2 level was no significant difference between 14 days and 21 days in the Sham group. Compared to the Sham group, the renal Bcl-2 level was decreased significantly in the UUO group at 14 days and 21 days (Figure 7C, 7D). Additionally, the Bcl-2 level was markedly increased in all the RAC treatment groups compared to the UUO group at 14 days and 21 days (Figure 7C, 7D).
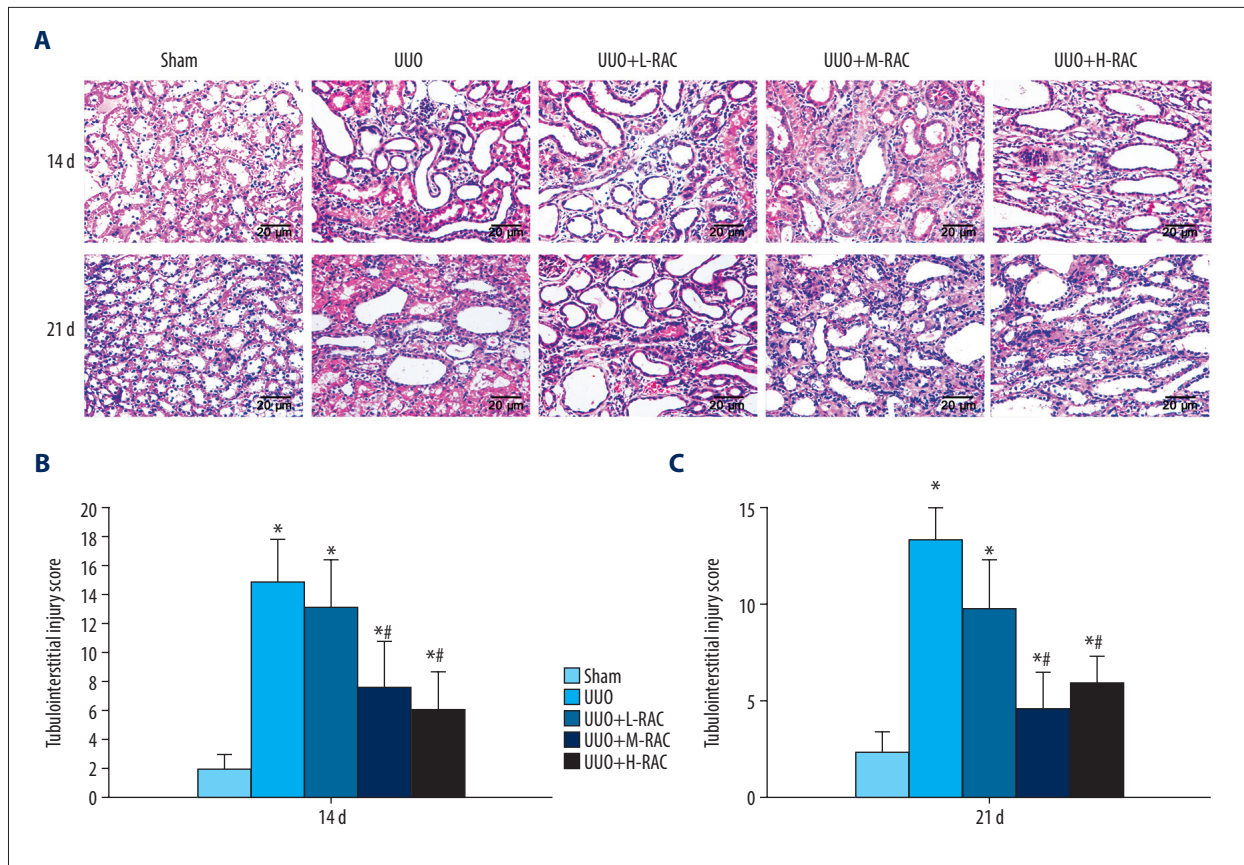
Figure 3. Effect of RAC on the histology of rat renal tissues. H&E staining was performed on the renal tissue slices. (**A**) Representative images (scale bar=20 μm) of H&E staining of rat renal tissue after 14 days and 21 days of UUO or sham-operation treatment. The tubulointerstitial injury scores of 14 days (**B**) and 21 days (**C**) from each group is shown. Data are presented as means±SD (n=10 in each group). * $P<0.05$ compared to the Sham group. # $P<0.05$ compared to UUO group. All results were assessed by 3 independent experiments. RAC – rhubarb and astragalus capsule; H&E – hematoxylin and eosin; UUO – unilateral ureteral obstruction; SD – standard deviation.

The renal Bcl-2 levels in all the RAC treatment groups were significantly increased at 21 days compared to 14 days ($P<0.05$).

RAC decreased the renal TGF-β1 level induced by UUO

Immunohistochemistry was used to detect the renal TGF-β1 level and found that TGF-β1 was mainly expressed in the cytoplasm of renal tubular epithelial cells. Compared to the Sham group, the TGF-β1 level was significantly increased in the UUO group at 14 days and 21 days (Figure 8A, 8C). Besides, the renal TGF-β1 level was markedly decreased in the UUO+M-RAC group and the UUO+H-RAC group compared to the UUO group at 14 days (Figure 8A, 8C). It was reduced significantly in all the RAC treatment groups compared to the UUO group at 21 days (Figure 8A, 8C).

At 14 days and 21 days, the TGF-β1 level was significantly lower in the UUO+M-RAC group and the UUO+H-RAC group than in the UUO+L-RAC group ($P<0.05$). The TGF-β1 level in

UUO+H-RAC group at 21 days was significantly lower than that at 14 days ($P<0.05$).

RAC decreased the renal p38 MAPK level induced by UUO

As shown in Figure 8B, compared with the Sham group, the positive-staining scores of p38 MAPK in the UUO group was significantly increased at 14 days and 21 days ($P<0.05$). At 14 days, the p38 MAPK level was significantly decreased in the UUO+M-RAC group and the UUO+H-RAC group compared to the UUO group (Figure 8B, 8D). At 21 days, the p38 MAPK level was significantly decreased in all the RAC treatment groups compared to the UUO group (Figure 8B, 8D).

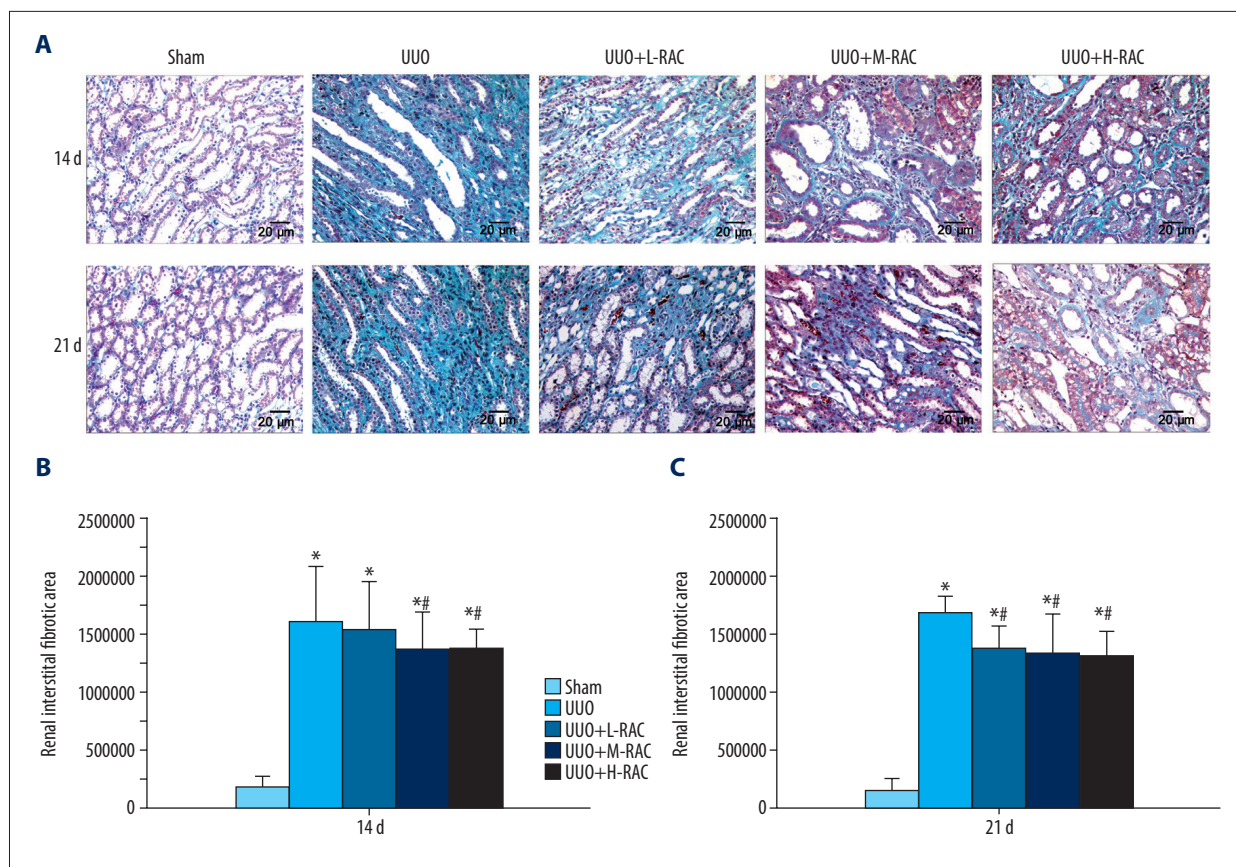The p38 MAPK level in the UUO+H-RAC group was significantly lower at 21 days than tat 14 days ($P<0.05$).

Figure 4. Detection of renal fibrosis in rat. Masson staining was performed on the renal tissue slices. (**A**) Representative images (scale bar=20 μm) of Masson stained of rat renal tissue after 14 days and 21 days of UUO or sham-operation treatment. The renal fibrosis areas of 14 days (**B**) and 21 days (**C**) from each group was measured and calculated using Image Proplus v6.0 software. Data are presented as means±SD (n=10 in each group). * *P*<0.05 compared to the Sham group. # *P*<0.05 compared to UUO group. All results were assessed by 3 independent experiments. UUO – unilateral ureteral obstruction; SD – standard deviation.

Discussion

RAC is a preparation that has been used clinically for many years and is used for the treatment of renal insufficiency, azotemia, uremia, etc., with excellent clinical results. Our previous study found that RAC can significantly improve renal function in patients with chronic kidney disease [7]. RAC contains rhubarb and astragalus, which are commonly used Chinese herbs in Chinese clinical practice. According to reports, the main pharmacologically active ingredients of rhubarb are aloe-emodin, rhein, emodin, and chrysophanol [27], whereas in astragalus the astragalus polysaccharides, astragalus saponins, astragalus flavonoid play therapeutic roles [28]. However, whether the chemical composition of RAC capsules is simply the mixture of the active ingredients of rhubarb and astragalus has not been tested in any publication. Here, our HPLC data showed that the RAC contained aloe-emodin, rhein, emodin, and chrysophanol, with the content amounts of 1.12, 2.25, 1.75, and 4.50 mg/g, respectively. The active ingredient of astragalus

could not be detected, probably because the astragalus content in RAC was too little.

Among these active ingredients of chemicals in RAC, emodin, rhein, and aloe-emodin, can functionally reduce kidney damages and improve the fibrosis of kidney tissue [15,29,30], while chrysophanol have been reported to as anti-inflammatory and anti-cardiac fibrosis [31]. In the present study, RAC treatment reduced the elevated levels of BUN and Scr in the blood, and urinary NAG, as well as renal tubulointerstitial injury score induced by UUO in experimental rats (Figure 2). Our previous clinical investigation has demonstrated that RAC could significantly reduce Scr, increased glomerular filtration rate and endogenous creatinine clearance in patients with chronic kidney disease [7]. Combining these findings in clinic and *in vivo* experiment using a rat model, it is suggested that the RAC could attenuate renal damage and protect normal renal functions by the synergic action of its main chemical components including emodin and rhein.
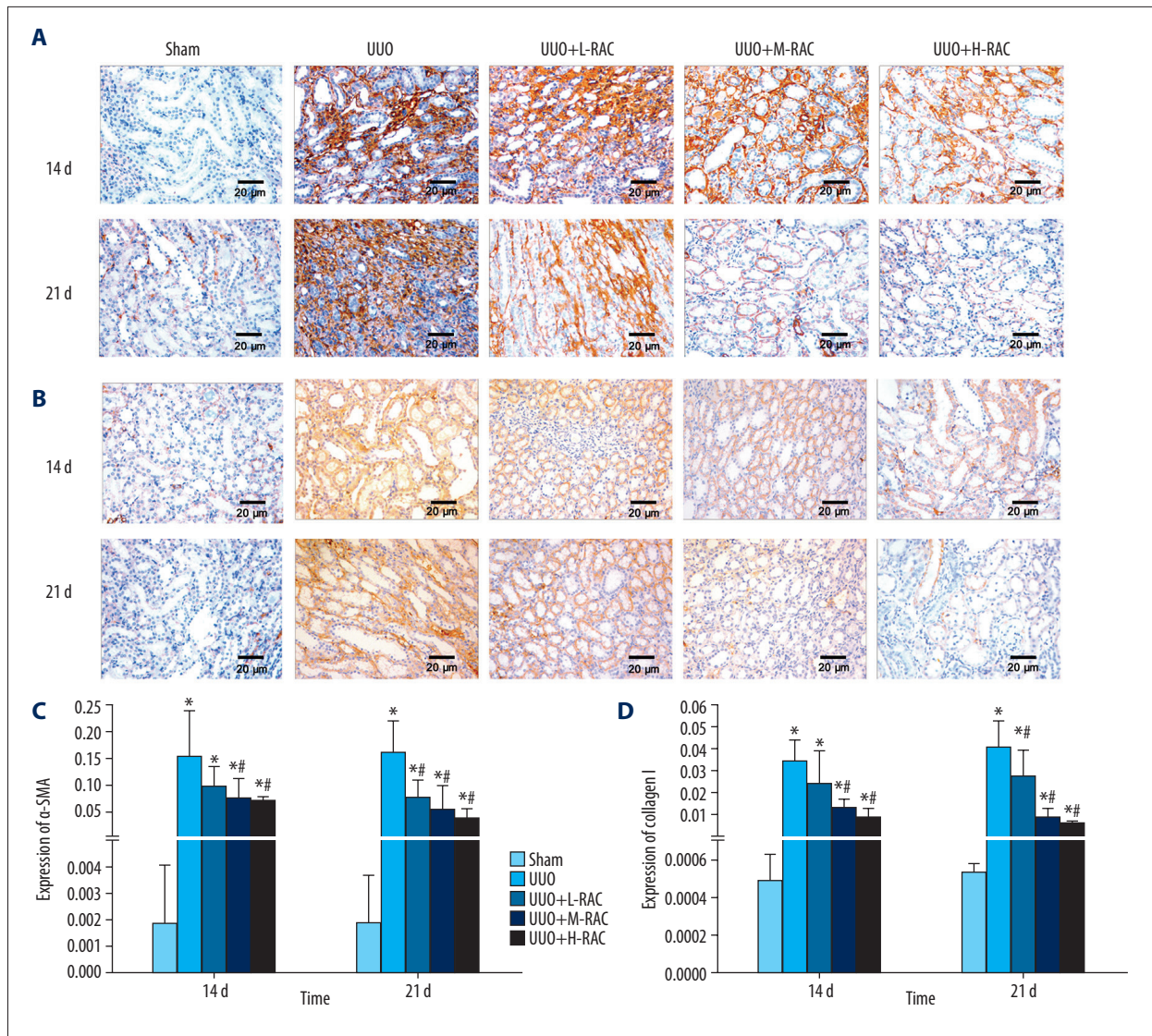
Figure 5. Effect of RAC on the expression of α-SMA and collagen I in rat renal tissues. Immunohistochemical staining was performed on the renal tissue slices to detect α-SMA or TGF-β1 expression. Representative images (scale bar=20 μm) of anti-α-SMA antibody (**A**) and anti-collagen I antibody (**B**) immunohistochemically stained renal tissue sections from Sham group, UUO group, UUO+L-RAC group, UUO+M-RAC group, and UUO+H-RAC group of rats. The protein expression levels of α-SMA (**C**) and collagen I (**D**) from each group was quantitated by measuring the integrated optical density (IOD) of the positively stained areas using Image Proplus v6.0 software. Data are presented as means±SD. * $P<0.05$ represents a statistically significant difference compared to the Sham group, and # $P<0.05$ represents a statistically significant difference compared to UUO group. Three independent experiments assessed all results. TGF – transforming growth factor; UUO – unilateral ureteral obstruction; SD – standard deviation.

It is known that long-term kidney damage and inflammation can trigger fibrotic lesions that largely impair renal functions. To analyze the effect of RAC on rescue renal function, we measure the level of fibrosis in renal tissue of rats among different treatment groups, according to the experiment design. The Masson's trichrome staining result showed that rat kidney from both the UUO model groups but not the Sham group, displayed positive stained area, suggesting the presence

of fibrosis. By comparing the area of fibrotic renal interstitial, we found that the level of fibrosis in the RAC-treated UUO rats was less severe than that in the untreated UUO rats. Myofibroblasts (Myof) are thought to be the primary cell type that produces extracellular matrix (ECM). Excessive deposition of ECM is known to be responsible for renal interstitial fibrosis [32]. Collagen I is the main component of ECM, and α-SMA is a marker protein for myofibroblasts activation. Fibrosis can
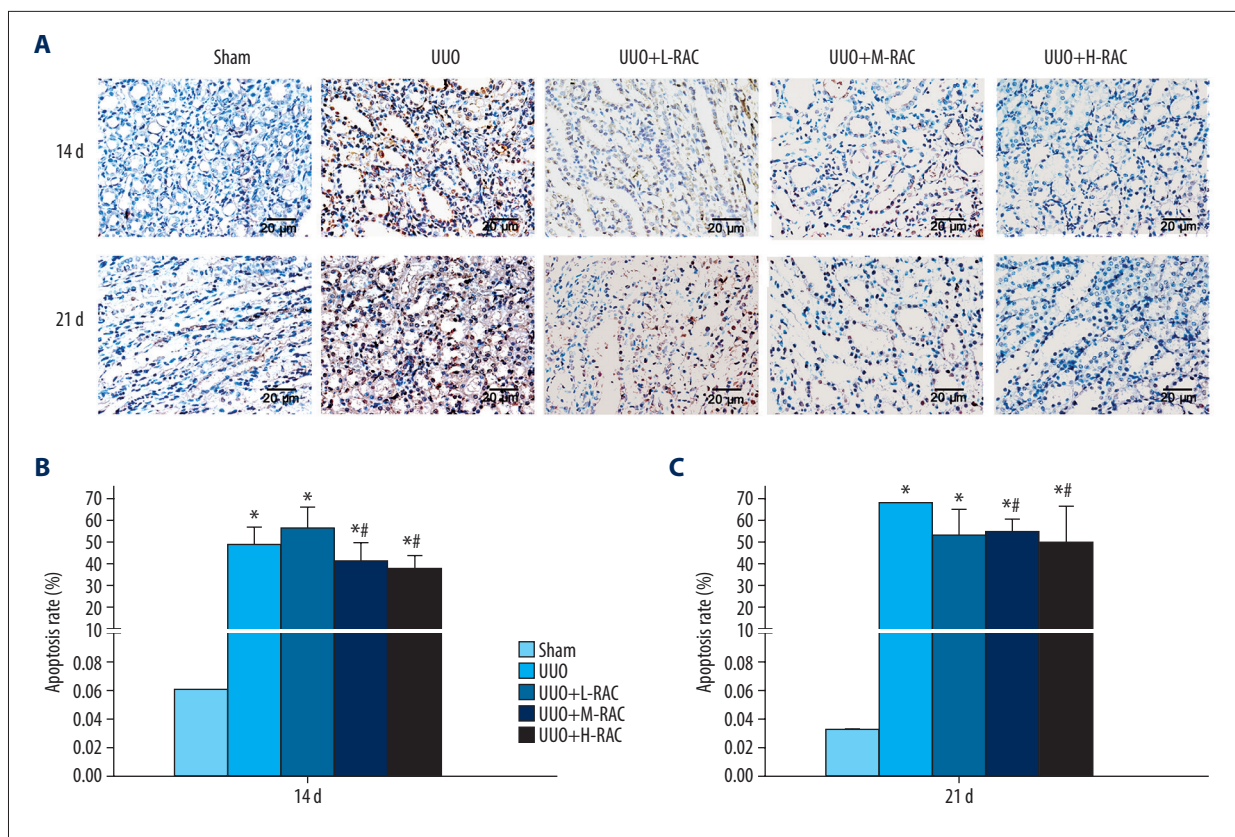
Figure 6. Detection of renal cell apoptosis by TUNEL assay. (**A**) Representative images (scale bar=20 µm) of TUNEL stained rat renal tissue after 14 days and 21 days of UUO or Sham treatment. The renal cell apoptosis rate of 14 days (**B**) and 21 days (**C**) from each group is shown. Data are presented as means±SD (n=10 in each group). * *P*<0.05 compared to the Sham group. # *P*<0.05 compared to UUO group. All results were assessed by 3 independent experiments. UUO – unilateral ureteral obstruction; SD – standard deviation.

be improved by inhibiting the expressions of α-SMA and collagen I [33]. Since the important roles of collagen I and α-SMA in ECM, we also determined the expression of these 2 factors in renal tissue of rats. Immunohistochemical staining of anti-α-SMA and anti-collagen I antibodies showed that, the levels of α-SMA and collagen I in renal tissues increased significantly in rats from the UUO model group. It was reported that rhubarb, one of the components of RAC, can reduce renal interstitial fibrosis [18]. Aloe-emodin and emodin, some of the active ingredients of RAC, have also been reported to inhibit the productions of α-SMA and collagen I [34,35]. Thus, the function of RAC treatment to reduce kidney damage may possible through alleviating renal interstitial fibrosis, as well as reducing the expression of α-SMA and collagen I.

Then we turned to ask if the RAC components were able to relieve the apoptosis of renal tubular cells. Severe apoptosis of renal tubular epithelial cells can induce tubular atrophy and renal interstitial fibrosis, while the inhibition of renal tubular cell apoptosis delays fibrosis [36,37]. Apoptosis can be initiated by the enhancing cell reactivity to the death signal when

the pro-apoptotic protein Bax is overexpressed in the cells. Conversely, when the anti-apoptotic protein Bcl-2 is overexpressed, it can inhibit apoptosis by directly binding to Bax and inhibiting Bax activation [38]. Therefore, the expression relation of the ratio between Bcl-2 and Bax is the key to decide the survival of cells. In our study, the results of TUNEL staining and western blotting clearly revealed that UUO induced renal tubular epithelial cells apoptosis, and RAC treatment was found to reduce the level of renal tubular epithelial cells apoptosis in the UUO rats, according to the percentage of apoptotic renal cells as well as the rate of Bcl-2 versus Bax expression. The majority of RAC contents, rhubarb and astragalus, further consisting of rhein, emodin, and other ingredients, has the bioactivity of anti-apoptosis. The emodin has been reported to inhibit cisplatin-induced renal tubular cells apoptosis in rats [39], whereas rhein and astragalus extract also display protective effects on cells against apoptosis [40,41]. In consistence of the study performed by Chen et al. [42], the anti-apoptotic effect of the emodin may be related to the upregulation of Bcl-2 and downregulation of Bax expression. Our results, therefore, suggest that RAC attenuates renal interstitial
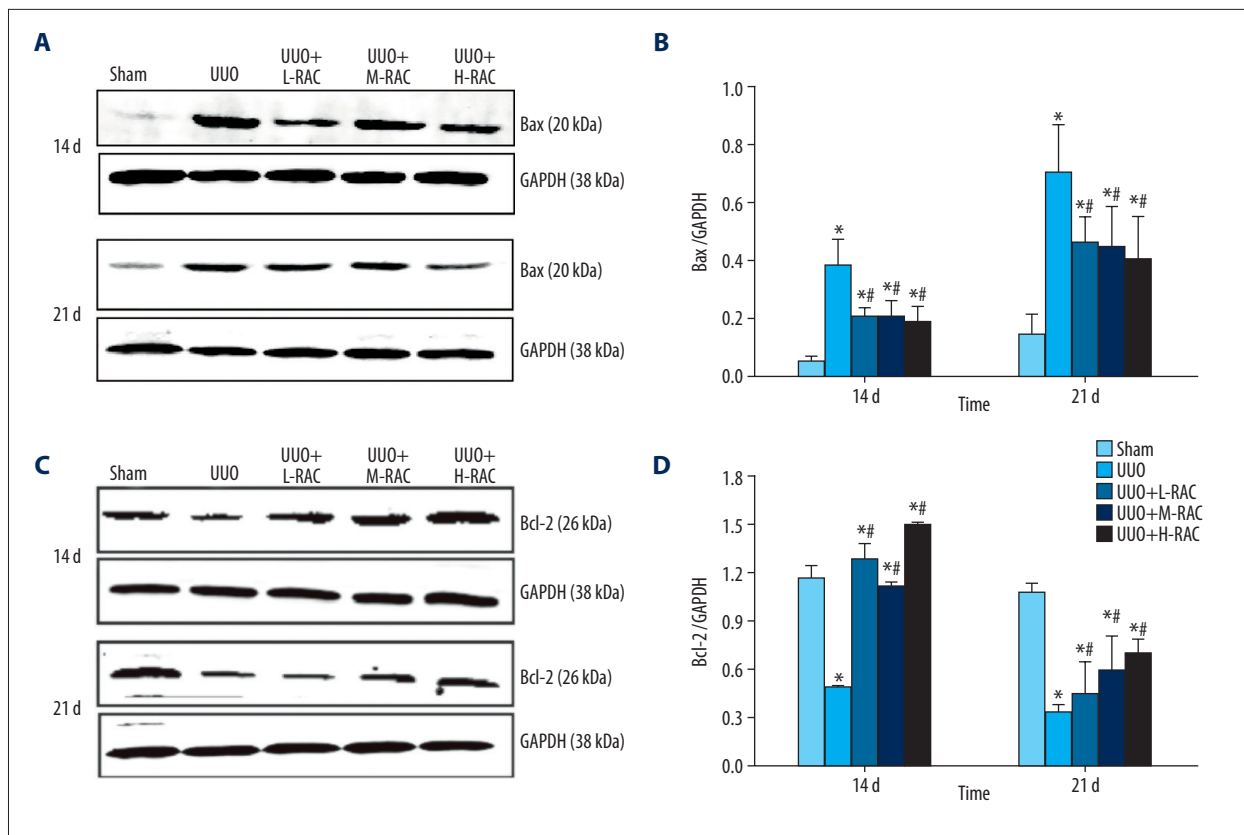
Figure 7. Effect of RAC on the expression of Bax and Bcl-2 proteins in rat renal tissues detected by immunoblotting. The total protein was extracted from the renal tissue sample from each group. Equal amounts of proteins were separated by western-blotting analyses. The expression of Bax (**A**) and Bcl-2 (**C**) protein were determined by using rabbit-anti-rat Bax and rabbit-anti-rat Bcl-2 antibodies, respectively. The result of western blotting was then quantitated by calculating and analyzing the gray image values. The relative expression of (**B**) Bax and (**D**) Bcl-2 in renal tissues from Sham, UUO, UUO+L-RAC, UUO+M-RAC, and UUO+H-RAC groups of rats are shown. Data are presented as means±SD (n=10 in each group). * $P<0.05$ compared to the Sham group. # $P<0.05$ compared to the UUO group. All results were assessed by 3 independent experiments. RAC – rhubarb and astragalus capsule; TGF – transforming growth factor; UUO – unilateral ureteral obstruction; SD – standard deviation.

fibrosis through the reduction of the apoptosis of renal tubular cells, where the correlation of the Bcl-2/Bax ratio may be highly involved.

Understanding the potential targets and signal pathways for RAC contents is extremely important to investigate the therapeutic mechanisms for RAC. Our immunohistochemistry data showed increased protein expression levels of TGF-β1 and p38 MAPK in renal tissues of UUO rats rather than Sham control, while RAC treatment significantly reduced the expression of both proteins comparing with the untreated group of the UUO rats. TGF-β1 is a crucial mediator in the progression of the process of fibrosis [43], and it can induce renal fibrosis via activation of myofibroblasts [44]. p38 MAPK is one of the noncanonical signaling pathways of TGF-β1. TGF-β1 activates the downstream signaling pathway MKK3-p38 MAPK cascade by activating TAK1, which ultimately leads to fibrosis [45,46]. Moreover, administrating of TGF-β1 or activation of p38 MAPK is capable to induce apoptosis

and aggravates tissue fibrosis [47,48]. In contrast, downregulation of the TGF-β1 limits or even reverses fibrosis [44]. There was also study showed that the blocking of p38MAPK could be effective in reducing renal fibrosis [12]. Therefore, the measurement of these 2 factors should be able to reflect the outcome of renal fibrosis after drug treatment. Here, the reduced levels of TGF-β1 and p38 MAPK in rat kidneys after receiving RAC treatment, has again confirmed the key role of TGF-β1/p38 MAPK cascading signaling during renal fibrosis, which has a strong correlation with the RAC potency against fibrosis in kidney. In addition, the rhubarb and astragalus, which are the main components of RAC, have been reported to downregulate the expression of TGF-β1 [18,21] and p38 MAPK [49–51] *in vivo* and *in vitro*. Their chemical ingredients, such as emodin and chrysophanol, are also found to inhibit the overexpression of TGF-β1 or p38 MAPK [52,53]. So, the supposed mechanism that active components of RAC improves renal interstitial fibrosis, may include the regulation of TGF-β1/p38 MAPK-related signaling pathway.
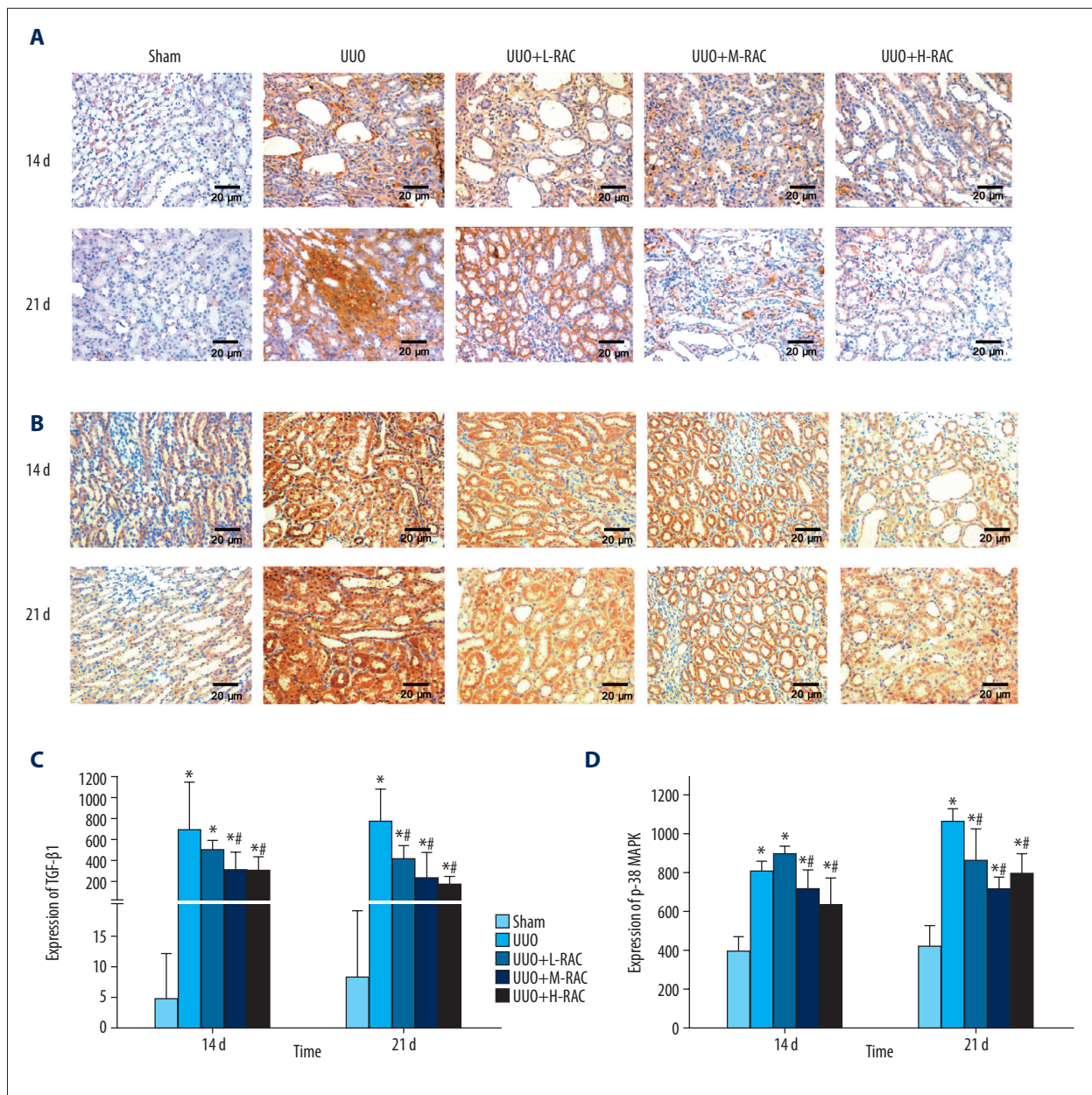
Figure 8. Effect of RAC on the expression of TGF-β1 and p38 MAPK in rat renal tissues. Immunohistochemical staining was performed on the renal tissue slices to detect TGF-β1 (**A**) or p38 MAPK (**B**) expression. Representative images (scale bar=20 μm) of anti-TGF-β1 antibody and anti-p38 MAPK antibody immunohistochemically stained renal tissue sections from Sham group, UUO group, UUO+L-RAC group, UUO+M-RAC group, and UUO+H-RAC group of rats. The protein expression levels of TGF-β1 (**C**) and p38 MAPK (**D**) from each group was quantitated by measuring the integrated optical density (IOD) of the positively stained areas using Image Proplus v6.0 software. Data are presented as means±SD. * $P<0.05$ represents a statistically significant difference compared to the Sham group, and # $P<0.05$ represents a statistically significant difference compared to the UUO group. Three independent experiments assessed all results. RAC – rhubarb and astragalus capsule; TGF – transforming growth factor; UUO – unilateral ureteral obstruction; SD – standard deviation.

Conclusions

Our present study, for the first time, demonstrates the anti-fibrotic potency of RAC against UUO-induced renal interstitial fibrosis in a rat model, which may be possibly due to the inhibition of renal tubular epithelial cells from apoptosis through regulating TGF-β1/p38 MAPK pathway. This work provides references and lays a solid foundation for any further investigation and application of RAC in the field of kidney disease treatment.

Limitations of study

There were some limitation to this research. The present study was based on an *in vivo* study as an extension of our previous clinical investigation. To fully explain the underlying mechanisms of anti-apoptotic effect for RAC, a series of prospectively designed *in vitro* experiments on renal tubular epithelial cells are still necessary in future.

Conflicts of interest

None.

References:

1. Ene-lordache B, Perico N, Bikbov B et al: Chronic kidney disease and cardiovascular risk in six regions of the world (ISN-KDDC): A cross-sectional study. Lancet Glob Health, 2016; 4: e307-19

2. Li X, Ma M, Zhang X et al: Ethanol extract of gardenia fruit alleviates renal interstitial fibrosis induced by unilateral ureteral obstruction in rats. Exp Ther Med, 2017; 14: 1381–88

3. Chen H, Xu Y, Yang Y et al: Shenqiwan ameliorates renal fibrosis in rats by inhibiting TGF-β1/Smads signaling pathway. Evid Based Complement Alternat Med, 2017; 2017: 7187038

4. Liu W, Lin S, Cai Q et al: Qingxuan Jiangya decoction mitigate renal interstitial fibrosis in spontaneously hypertensive rats by regulating transforming growth factor-β1/Smad signaling pathway. Evid Based Complement Alternat Med, 2017; 2017: 1576328

5. Zeyad A, Kimberly CC, Yao MC, Francis CPL: Predicting the content of anthraquinone bioactive in Rhei rhizome (Rheum officinale Baill.) with the concentration addition model. Saudi Pharm J, 2019; 27(1): 25–32

6. Simona A, Rosario R, Andrea Q et al: *Astragalus membranaceus* extract attenuates inflammation and oxidative stress in intestinal epithelial cells via NF- B activation and Nrf2 response. Int J Mol Sci, 2018; 19(3): 800

7. Cai GZ, Zhong XB, Yang YF et al: [Clinical study of RAC Capsule in the treatment of renal insufficiency.] Chinese Pharmacy, 2017; 28, 1934–37 [in Chinese]

8. Guo J, Wu W, Sheng M et al: [Amygdalin inhibits renal fibrosis in chronic kidney disease.] Mol Med Rep, 2013; 7: 1453–57 [in Chinese]

9. Wang S, Sun Z, Yang S et al: CTRP6 inhibits cell proliferation and ECM expression in rat mesangial cells cultured under TGF-β1. Biomed Pharmacother, 2018; 97: 280–85

10. Silva TA, Ferreira LFC, Pereira MCS, Calvet CM: Differential role of TGF-β in extracellular matrix regulation during trypanosoma cruzi-host cell interaction. Int J Mol Sci, 2019; 20: 4836

11. Sun L, Xiu M, Wang SH et al: Lipopolysaccharide enhances TGF-β1 signalling pathway and rat pancreatic fibrosis. J Cell Mol Med, 2018; 22: 2346–56

12. Wang DP, Gina MW, Yin P et al: Inhibition of p38 MAPK attenuates renal atrophy and fibrosis in a murine renal artery stenosis model. Am J Physiol Renal Physiol, 2013; 304: F938–47

13. Liu ZQ, Xue LX, Liu ZC et al: Tumor necrosis factor-like weak inducer of apoptosis accelerates the progression of renal fibrosis in lupus nephritis by activating SMAD and p38 MAPK in TGF-β1 signaling pathway. Mediators Inflamm, 2016; 2016: 8986451

14. Xie X, Li Z, Pi M et al: [Down-regulation of p38 MAPK and collagen by 1 25-(OH)2-VD3 in rat models of diabetic nephropathy.] Xi Bao Yu Fen Zi Mian Yi Xue Za Zhi, 2016; 32(7): 931–35. [in Chinese]

15. Tu Y, Gu L, Chen D et al: Rhein inhibits autophagy in rat renal tubular cells by regulation of AMPK/mTOR signaling. Sci Rep, 2017; 7: 43790

16. Li H, Yang T, Zhou H et al: Emodin combined with nanosilver inhibited sepsis by anti-inflammatory protection. Front Pharmacol, 2017; 7: 536

17. Tsao YT, Kuo CY, Kuan YD et al: The extracts of *Astragalus membranaceus* inhibit melanogenesis through the ERK signaling pathway. Int J Med Sci, 2017; 14: 1049–53

18. Zhang ZH, Li MH, Liu D et al: Rhubarb protect against tubulointerstitial fibrosis by inhibiting TGF-β/Smad pathway and improving abnormal metabolome in chronic kidney disease. Front Pharmacol, 2018; 9: 1029

19. Zhang ZH, Vaziri ND, Wei F et al: An integrated lipidomics and metabolomics reveal nephroprotective effect and biochemical mechanism of Rheum officinale in chronic renal failure. Sci Rep, 2016; 6: 22151

20. Wang J, Fang H, Dong B et al: Effects of free anthraquinones extract from the rhubarb on cell proliferation and accumulation of extracellular matrix in high glucose cultured-mesangial cells. Korean J Physiol Pharmacol, 2015; 19: 485–89

21. Li Z, Zhang L, He W et al: *Astragalus membranaceus* inhibits peritoneal fibrosis via monocyte chemoattractant protein (MCP)-1 and the transforming growth factor-β (TGF-β1) pathway in rats submitted to peritoneal dialysis. Int J Mol Sci, 2014; 15: 12959–71

22. Ren GX, Li L, Hu HJ et al: Influence of the environmental factors on the accumulation of the bioactive ingredients in Chinese rhubarb products. PLoS One, 2016; 11: e0154649

23. Zhou RJ, Chen HJ, Chen JP et al: Extract from *Astragalus membranaceus* inhibit breast cancer cells proliferation via PI3K/AKT/mTOR signaling pathway. BMC Complement Altern Med, 2018; 18: 83

24. Mei ZG, Tan LJ, Wang JF et al: Fermented Chinese formula Shuan-Tong-Ling attenuates ischemic stroke by inhibiting inflammation and apoptosis. Neural Regen Res, 2017; 12: 425–32

25. Liang XY, Yang YF, Huang ZG et al: Panax notoginseng saponins mitigate cisplatin induced nephrotoxicity by inducing mitophagyvia HIF-1α. Oncotarget, 2017; 8: 102989–3003

26. Zhang C, Zhou Y, Zhou Y et al: Regulation of eIF2α expression and renal interstitial fibrosis by resveratrol in rat renal tissue after unilateral ureteral obstruction. Ren Fail, 2016; 38: 622–28

27. Cai Y, Sun M, Xing J, Corke H: Antioxidant phenolic constituents in roots of Rheum officinale and *Rubia cordifolia*: structure-radical scavenging activity relationships. J Agric Food Chem, 2004; 52: 7884–90

28. Li ZX, Zhao GD, Xiong W et al: Immunomodulatory effects of a new whole ingredients extract from Astragalus: A combined evaluation on chemistry and pharmacology. Chin Med, 2019; 14: 12

29. Wang XT, Sun XJ, Li C et al: Establishing a cell-based high-content screening assay for TCM compounds with anti-renal fibrosis effects. Evid Based Complement Alternat Med, 2018; 2018: 7942614

30. Dou F, Liu Y, Liu L et al: Aloe-emodin ameliorates renal fibrosis via inhibiting PI3K/Akt/mTOR signaling pathway *in vivo* and *in vitro*. Rejuvenation Res, 2019; 22: 218–29

31. Lian YG, Xia XJ, Zhao HY, Zhu YF: The potential of chrysophanol in protecting against high fat-induced cardiac injury through Nrf2-regulated anti-inflammation, anti-oxidant and anti-fibrosis in Nrf2 knockout mice. Biomed Pharmacother, 2017; 93: 1175–89

32. Xie XS, Zuo C, Zhang ZY et al: [Investigate the effects of compound radix notoginseng on renal interstitial fibrosis and kidney-targeting treatment.] Sichuan Da Xue Xue Bao Yi Xue Ban, 2012; 43: 28–33 [in Chinese]

33. Yang D, Li L, Qian S, Liu L: Evodiamine ameliorates liver fibrosis in rats via TGF-β1/Smad signaling pathway. J Nat Med, 2018; 72: 145–54

34. Woo SW, Nan JX, Lee SH et al: Aloe emodin suppresses myofibroblastic differentiation of rat hepatic stellate cells in primary culture. Pharmacol Toxicol, 2002; 90: 193–98

35. Zhao XA, Chen G, Liu Y et al: Emodin alleviates liver fibrosis of mice by reducing infiltration of Gr1hi monocytes. Evid Based Complement Alternat Med, 2018; 2018: 5738101

36. Ren Y, Du C, Yan L et al: CTGF siRNA ameliorates tubular cell apoptosis and tubulointer-stitial fibrosis in obstructed mouse kidneys in a Sirt1-independent manner. Drug Des Devel Ther, 2015; 9: 4155–71

37. Li HY, Xu YX, Zhang Q et al: Microvesicles containing miR-34a induce apoptosis of proximal tubular epithelial cells and participate in renal interstitial fibrosis. Exp Ther Med, 2019; 17: 2310–16

This work is licensed under Creative Common Attribution-NonCommercial-NoDerivatives 4.0 International (CC BY-NC-ND 4.0)

e920720-13

Indexed in: [Current Contents/Clinical Medicine] [SCI Expanded] [ISI Alerting System]
[ISI Journals Master List] [Index Medicus/MEDLINE] [EMBASE/Excerpta Medica]
[Chemical Abstracts/CAS]

38. Lindqvist LM, Heinlein M, Huang DC, Vaux DL: Prosurvival Bcl-2 family members affect autophagy only indirectly, by inhibiting Bax and Bak. Proc Natl Acad Sci USA, 2014; 111: 8512–17

39. Liu H, Gu LB, TuY et al: Emodin ameliorates cisplatin-induced apoptosis of rat renal tubular cells *in vitro* by activating autophagy. Acta Pharmacol Sin, 2016; 37: 235–45

40. Liu J, Chen ZH, Zhang YJ et al: Rhein protects pancreatic β-cells from dynamin-related protein-1-mediated mitochondrial fission and cell apoptosis under hyperglycemia. Diabetes, 2013; 62: 3927–35

41. Li HT, Zhou XQ, Wu M et al: The cytotoxicity and protective effects of *Astragalus membranaceus* extracts and butylated hydroxyanisole on hydroxyl radical-induced apoptosis in fish erythrocytes. Anim Nutr, 2016; 2: 376–82

42. Chen H, Huang RS, Yu XX et al: Emodin protects against oxidative stress and apoptosis in HK-2 renal tubular epithelial cells after hypoxia/reoxygenation. Exp Ther Med, 2017; 14: 447–52

43. Guo J, Fang Y, Jiang F et al: Neohesperidin inhibits TGF-β1/Smad3 signaling and alleviates bleomycin-induced pulmonary fibrosis in mice. Eur J Pharmacol, 2019; 2: 172712

44. Chen J, Li D: Telbivudine attenuates UUO-induced renal fibrosis via TGF-β/Smad and NF-κB signaling. Int Immunopharmacol, 2018; 55: 1–8

45. Kim SI, Kwak JH, Zachariah M et al: TGF-beta-activated kinase 1 and TAK1-binding protein 1 cooperate to mediate TGF-beta1-induced MKK3-p38 MAPK activation and stimulation of type I collagen. Am J Physiol Renal Physiol, 2007; 292: F1471–78

46. Kye-Im J, Richard P, Patricia JS, Krystel RH: Antifibrotic actions of peroxisome proliferator-activated receptor γ ligands in corneal fibroblasts are mediated by β-catenin-regulated pathways. Am J Pathol, 2017; 187: 1660–69

47. Rouschop KM, Claessen N, Pals ST et al: CD44 disruption prevents degeneration of the capillary network in obstructive nephropathy via reduction of TGF-beta1-induced apoptosis. J Am Soc Nephrol, 2006; 17: 746–53

48. Chen L, Jiang K, Chen H et al: Deguelin induces apoptosis in colorectal cancer cells by activating the p38 MAPK pathway. Cancer Manag Res, 2018; 11: 95–105

49. Ma YS, Hsiao YP, Lin JHvCrude extract of *Rheum palmatum* L inhibits migration and invasion of LS1034 human colon cancer cells acts through the inhibition of matrix metalloproteinase-2/-9 by MAPK signaling. Environ Toxicol, 2015; 30: 852–63

50. Xiang Z, Sun H, Cai X et al: The study on the material basis and the mechanism for anti-renal interstitial fibrosis efficacy of rhubarb through integration of metabonomics and network pharmacology. Mol Biosyst, 2015; 11: 1067–78

51. Qin Q, Niu J, Wang Z et al: *Astragalus membranaceus* inhibits inflammation via phospho-p38 mitogen-activated protein kinase (MAPK) and nuclear factor (NF)-κB pathways in advanced glycation end product-stimulated macrophages. Int J Mol Sci, 2012; 13: 8379–87

52. Guan RJ, Wang X, Zhao XM et al: Emodin ameliorates bleomycin-induced pulmonary fibrosis in rats by suppressing epithelial-mesenchymal transition and fibroblast activation. Sci Rep, 2016; 6: 35696

53. Selim NM, Elgazar AA, Abdel-Hamid NM et al: Chrysophanol, physcion, hesperidin and curcumin modulate the gene expression of pro-inflammatory mediators induced by LPS in HepG2: *In silico* and molecular studies. Antioxidants (Basel), 2019; 3: 8: 371